The Journal of Immunology

Dynamics of Human Respiratory Virus-Specific CD8 $^{+}$ T Cell Responses in Blood and Airways during Episodes of Common Cold

Jojanneke Heidema, John W. A. Rossen, Michaël V. Lukens, Marianne S. Ketel, Eva Scheltens, Mariette E. G. Kranendonk, Wendy W. C. van Maren, Anton M. van Loon, Henny G. Otten, Jan L. L. Kimpen and Grada M. van Bleek

J Immunol 2008; 181:5551-5559; ;
doi: 10.4049/jimmunol.181.8.5551
http://www.jimmunol.org/content/181/8/5551

The Journal of Immunology is published twice each month by
The American Association of Immunologists, Inc.,
1451 Rockville Pike, Suite 650, Rockville, MD 20852

Print ISSN: 0022-1767 Online ISSN: 1550-6606.

Dynamics of Human Respiratory Virus-Specific CD8$^+$ T Cell Responses in Blood and Airways during Episodes of Common Cold[1]

Jojanneke Heidema,* John W. A. Rossen,[2†] Michaël V. Lukens,[2*] Marianne S. Ketel,* Eva Scheltens,* Mariette E. G. Kranendonk,* Wendy W. C. van Maren,* Anton M. van Loon,† Henny G. Otten‡, Jan L. L. Kimpen,* and Grada M. van Bleek[3]*

We determined the dynamics of CD8$^+$ T cells specific for influenza virus and respiratory syncytial virus in blood and tracheostoma aspirates of children during the course of respiratory infections. We showed that during localized respiratory infections the ratio of activated effector CD8$^+$ T cells to resting memory/naive CD8$^+$ T cells in peripheral blood increased significantly. Furthermore, the number of effector/memory T cells specific for respiratory viruses declined in blood and increased in the airways, suggesting that these T cells redistributed from blood to airways. T cells specific for the infecting virus were present in the airways for longer periods at increased levels than nonspecifically recruited bystander T cells. After clearance of the infection, the ratio of resting memory and naive CD8$^+$ T cells normalized in peripheral blood and also memory T cell numbers specific for unrelated viruses that declined during the infection due to bystander recruitment were restored. Taken together, these results showed a significant systemic T cell response during relatively mild secondary infections and extensive dynamics of virus-specific and nonspecific Ag-experienced T cells. *The Journal of Immunology,* **2008, 181: 5551–5559.**

Antiviral CD8$^+$ T cells are important for resolution of both primary and secondary viral infections. However, for respiratory infections caused by respiratory syncytial virus (RSV)[4] and influenza virus, protective T cell-mediated immunity decreases over time (1–3). The respiratory tract is one of the largest surface areas of the body and effective immune surveillance is required to prevent damage caused by infectious and environmental Ags. Even in the absence of local infections in the lung, effector/memory T cells are effectively attracted to this peripheral site by continuous chemokine-mediated T cell recruitment from the vasculature into the tissue (4). This process of effector cell recruitment is enhanced during infections when local chemokine production is up-regulated. When infections are cleared, substantial numbers of T cells remain detectable in the lung tissue and airways (5, 6). The role of different T cell populations that are recruited into lung tissue and the airways in the process of viral eradication is still unclear, as is the mechanism by which the balance between the different T cell populations is reinstilled in peripheral blood after viral clearance.

Most insight into the dynamics of CD8$^+$ T cell responses during respiratory infections has come from studies in mice. In the mouse model, naive virus-specific CD8$^+$ T cells differentiate and gain the capacity to traffic into inflamed tissue during primary infection. Typically, proliferating T cells are first detected in the draining lymph nodes around day 4, from where they migrate to the lungs where they are found from day 6 onward (7). Peak responses are found in the tissue around days 8–10, while viral load declines as soon as CTLs appear (8). After resolution of the infection, the virus-specific T cell pool contracts and a small number of T cells survive and become long-lived memory T cells.

Upon secondary infection a three-phase defense has been suggested (9). The first phase is represented by effector/memory CD8$^+$ T cells that are already present in the lungs. Cytokines and chemokines are secreted by these cells to create a proinflammatory milieu that attracts other immune cells. During the second phase a wave of nonproliferating T cells is recruited to the lung around day 4 in a non-Ag-specific manner. Memory T cells specific for the infecting virus as well as nonspecific bystanders are recruited. Bystanders do not proliferate and are deleted by apoptosis or phagocytosis. The third phase consists of Ag-specific effector cells that are derived from reactivated memory cells in the draining lymph nodes (10, 11).

Few data have been published on the human host. A recent study has shown that CD8$^+$ T cells specific for respiratory infections could be detected in lung tissue of elderly people that had no symptoms of infection at the time tissue biopsies were taken (12). There was a relative enrichment of CD8$^+$ T cells specific for influenza virus and RSV in the lung tissue compared with blood that was not found for EBV. These cells had progressed to a highly differentiated phenotype and were IL-7 receptor (CD127)-positive, reflecting their memory status. The relationship between airway and tissue resident CD8$^+$ T cells and their relative contribution to viral clearance is currently unclear. In mice it was found that effector/memory cells were predominantly recruited to the airways

*Division of Paediatrics, Wilhelmina Children's Hospital, †Department of Virology, and ‡Department of Immunology, University Medical Center, Utrecht, the Netherlands

Received for publication October 9, 2007. Accepted for publication August 8, 2008.

The costs of publication of this article were defrayed in part by the payment of page charges. This article must therefore be hereby marked *advertisement* in accordance with 18 U.S.C. Section 1734 solely to indicate this fact.

[1] This work was supported by the Wilhelmina Research Fund.

[2] J.W.A.R. and M.V.L. equally contributed to this work.

[3] Address correspondence and reprint requests to Dr. Grada van Bleek, Department of Pediatric Immunology, The Wilhelmina Children's Hospital, KE04.133.1, University Medical Center Utrecht, Lundlaan 6, 3584 CX Utrecht, The Netherlands. E-mail address: g.vanbleek@umcutrecht.nl

[4] Abbreviations used in this paper: RSV, respiratory syncytial virus; GzmB, granzyme B; moi, multiplicity of infection; RT, reverse transcriptase.

Table I. *Characteristics of tracheostoma patients*

Patient	Age (years)	HLA Type[a]	Underlying Disorder	Virus
1	2	A1	Subglottic stenosis	RSV
2	4	A1	Pierre Robin sequence	Rhinovirus
3	3	A3	Spina bifida aperta	RSV
4	3	—[b]	Trisomy 11	RSV
5	6	A3	Congenital muscle dystropy 1a	RSV
6	12	A2	Nemaline myopathy	Unknown
7	16	A1	Spina bifida aperta	Unknown
8	17	B7	Spina bifida aperta	Rhinovirus
9	5	A2, B7	Mitochondrial complex 1 deficiency	Rhinovirus → RSV → coronavirus → rhinovirus
10	1	A1, B7	Lunghypoplasia	Coronavirus → rhinovirus and human metapneumovirus → adenovirus, human metapneumovirus, and rhinovirus → influenza virus
11	2	—[b]	Unknown retardation	Rhinovirus
12	2	A2	Spinal cord lesion	Rhinovirus
13	14	A1	Spinal muscle dystrophy	Rhinovirus
14	7 mo	A1, A3, B7	Down syndrome	Unknown
15	1	A1	Crouzon syndrome	RSV

[a] HLA molecule used for tetramer studies.
[b] HLA type of these children did not include HLA-A1, HLA-A2, HLA-A3 or HLA-B7, the HLA types for which tetramers were available.

(13, 14). These cells did not divide locally, and the virus-specific CD8$^+$ T cell numbers declined in murine models around 6 mo after infection (3).

Information obtained in murine models may not always reflect the human situation. Using human pathogens like influenza virus and RSV in the mouse model and the difference in anatomy in the murine and human pulmonary circulation may lead to differences in the inflammatory milieu and in the in vivo trafficking of immune cells (15, 16). These differences may result in different populations of immune cells that contribute to the response. Therefore, we investigated the dynamics of human CD8$^+$ T cells specific for two respiratory viruses, RSV and influenza virus, in peripheral blood and tracheostoma aspirates of individuals during episodes of respiratory infections. We showed that during mild respiratory infections significant shifts in cell populations occurred in peripheral blood and airways. Both virus-specific and bystander CD8$^+$ T cells migrated to the lungs, and lower numbers of virus-specific effector/memory cells were detectable in the blood. Furthermore, the bystander response was more transient in the airways than was the virus specific response. In blood the level of bystander memory/effector cells reestablished at a level similar to that before the respiratory infection. This study shows for the first time the dynamics of CD8$^+$ T cell responses during mild local respiratory infections in humans.

Materials and Methods

Study population and sample collection

Fifteen patients with a tracheostoma between 6 mo and 18 years of age were included in the study during the winter season of 2005–2006 (Table I). Exclusion criteria were immune disorders and the use of immune suppressive medication. Blood samples were taken prior to or on day 1 of the first episode of common cold. In one patient with paralysis of the legs and absent pain perception, blood samples were drawn at all time points when tracheal aspirate was collected. Parents were asked to collect morning samples of tracheal aspirate on days 2, 5, 8, 15, 28, and 56 after the start of a common cold. During RSV or influenza virus infections, a seventh sample was collected on day 42. Samples were kept on ice during transport. All samples were processed within 4 h after collection.

Healthy blood donors were followed during the winter season. Twenty milliliters of heparinized blood samples were drawn, either once a week for a 10-wk period, or at two time points before and after onset of common cold symptoms and at one to four time points during clinical signs of a common cold. Nose and throat swabs for viral PCR were taken at all time points. PBMC were isolated by Ficoll-Paque gradient centrifugation (Pharmacia Biotech) and used immediately or stored in liquid nitrogen. Healthy blood donors and parents of patients gave their informed written consent. The study was approved by the Medical Ethical Committee of the University Medical Center, Utrecht.

Viruses

Human RSV strain A2 was propagated in HEp-2 cells, and the viral titer was determined by plaque assay. RSV was used at a multiplicity of infection (moi) of 5 in the ELISPOT assay. Influenza virus strain A/Nanchang/933/95, H3N2, was made in embryonated chicken eggs and used at a moi of 5 in the ELISPOT assay.

Real-time PCR

Tracheal aspirate samples or nose and throat swabs were evaluated for respiratory viruses by real-time PCR. After spiking of samples with murine encephalomyocarditis virus and phocine herpes virus, nucleic acids were extracted using the total nucleic acid protocol with the MagNA pure LC nucleic acid isolation system (Roche Diagnostics). Each sample was eluted in 200 μl of buffer, which was sufficient for all real-time PCR analyses. cDNA was synthesized by using MultiScribe reverse transcriptase (RT) and random hexamers (both from Applied Biosystems). Each 200 μl reaction mixture contained 80 μl of eluted RNA, 20 μl of 10× RT buffer, 5.5 mM $MgCl_2$, 500 μM of each deoxynucleoside triphosphate, 2.5 μM random hexamer, and 0.4 U of RNase inhibitor/μl (all from Applied Biosystems). After incubation for 10 min at 25°C, RT was conducted for 30 min at 48°C, followed by RT inactivation for 5 min at 95°C.

Detection of viral and atypical pathogens was performed in parallel, using real-time PCR assays specific for: RSV A and B, influenza virus A and B, parainfluenza virus 1–4, rhinoviruses, adenoviruses, human coronaviruses OC43, NL63, and 229E, human metapneumovirus, *Mycoplasma pneumoniae*, and *Chlamydia pneumoniae*. Real-time PCR procedures were performed as previously described (17). Briefly, samples were assayed in duplicate in a 25 μl reaction mixture containing 10 μl of cDNA, 12.5 μl 2× TaqMan Universal PCR master mix (Applied Biosystems), and 300–900 nM of the forward and reverse primers and 75–200 nM of each of the probes (together 2.5 μl). Efficient extraction and amplification was monitored through the internal control viruses (murine encephalomyocarditis virus (RNA virus) and phocine herpes virus (DNA virus)) (18).

HLA typing

To be able to perform HLA tetramer staining in fresh tracheal aspirate samples, immediate limited HLA typing was required. Therefore, 50 μl of whole blood was stained with a panel of HLA-specific Abs to be able to select the proper HLA tetrameric complexes to be used for T cell identification (IHB-Hu-037 for HLA-A1/A36, BB7.2 for HLA-A2, and IHB-Hu-035 for HLA-B7 were kindly supplied by Dr. A. Mulder, Leiden University Medical Center, Leiden, The Netherlands). After 30 min of incubation at room temperature, cells were labeled with FITC-conjugated Fab fragments (IgG1 for IHB-Hu-035, IgMκ for IHB-Hu-037, DAKO

F0315, and F0317, and IgG2b for BB7.2) and incubated for another 30 min. Erythrocytes were lysed using lysis buffer (BD Bioscience). Cells were analyzed by FACSCalibur flow cytometer and CellQuest software (BD Biosciences). HLA type of the patients was confirmed in a later stage by PCR-sequence-specific primers (SSP) using cultured EBV B cell lines of the patients. PCR-SSP was performed according to the instructions of the manufacturer (Biotest).

ELISPOT assay

Filtration plates (96-well; MAIPS4510; Millipore) were coated overnight with anti-IFN-γ coating Ab 1-D1K (100 μl, 15 μg/ml; Mabtech) in 0.1 M carbonate-bicarbonate buffer (pH 9.6) at 4°C. Before adding the PBMC, the plates were washed thoroughly with PBS and blocked for 1 h at 37°C with RPMI 1640 containing 10% FBS. Cells and virus (RSV or influenza virus both used at a moi of 5) were added to the wells in triplicate in a final volume of 200 μl of RPMI 1640 containing 10% FBS and penicillin and streptomycin. Cells were incubated at 37°C for 24 h in a humidified incubator. Cells were then removed by thorough washing in PBS, and 100 μl of detecting Ab 7-B6-1-biotin (Mabtech), diluted to 1 μg/ml in PBS-0.5% FBS, was added to the wells. After incubating 2 h at room temperature and washing (PBS), 100 μl (diluted 1/1000 in PBS-0.5% FBS), ExtraAvidine alkaline phosphatase conjugate (Sigma-Aldrich) was added and incubated for 1 h at room temperature. The plates were then washed in PBS, and 5-bromo-4-chloro-3-indolylphosphate-NBT substrate was added at 100 μl/well (Sigma-Aldrich, one tablet dissolved in 10 ml of H_2O). Spots were counted by an automated ELISPOT reader. Data were represented as the number of spots per 3×10^5 PBMC minus the background of unstimulated samples. In the mAb blocking experiments, we used culture supernatants of hybridomas B8.11.2 producing anti HLA-DR, SPVL3 producing anti HLA-DQ, and B7/21 producing anti HLA-DP.

CD8$^+$ T cell phenotyping

To maximize cell viability, tracheal aspirate samples were processed directly after sampling. Specimens were filtered through 70-μm cell strainers (Falcon, BD Biosciences) to remove mucus. Cells were washed in RPMI 1640 medium supplemented with penicillin and streptomycin and 10% FCS and blocked in FACS buffer containing 10% HPS for 30 min on ice. Cells were stained with the appropriate HLA-A1, HLA-A2, HLA-A3, or HLA-B7 tetramer. The allophycocyanin-conjugated HLA-B7 tetramer loaded with the RSV peptide NPKASLLSL ($NP_{306-314}$), the HLA-A1 tetramer loaded with the RSV peptide YLEKESIYY ($M_{229-237}$), the HLA-A3 tetramer loaded with the RSV-derived peptide RLPADVLKK ($M2_{151-159}$), and the HLA-A2 tetramer loaded with the influenza virus peptide GILG FVFTL ($M1_{58-66}$) were purchased from Sanquin. The HLA-A1 tetramer loaded with influenza NP-derived CTELKLSDY (NP_{44-52}) peptide was obtained from Proimmune.

After 20 min, cells were stained extracellular with different mAbs for another 20 min at room temperature. FITC-conjugated anti-CD8, anti-CD25, anti-CD27, anti-CD45RO, anti-CCR5, and anti-CD38; PE-conjugated anti-CD4, anti-CD8, anti-CD27, anti-CD28, anti-CD38, anti-CD45RO, HLA-DR, and anti-CCR7; PerCP-conjugated anti-CD8 and anti-HLA-DR; and allophycocyanin-conjugated anti-CD3, anti-CD8, and anti-CD28 were all purchased from BD Pharmingen, except for CD8-FITC (Sanquin) and CD127-PE (Immunotech). For intracellular staining, cells were permeabilized and fixed using FACS permeabilizing/fixation solution (Perm/Fix, BD Pharmingen). Cells were stained intracellular with FITC-conjugated Ki-67, FITC-perforin (both BD Pharmingen), PE-conjugated granzyme B (GzmB, Sanquin) or isotype control (BD Pharmingen) for 30 min at room temperature. Cells were washed twice in Perm/Wash and once in FACS buffer. For surface-stained samples, 7-aminoactinomycin D (BD Pharmingen) was added just before FACS analysis to visualize cell viability. Cell staining was analyzed on a FACSCalibur using CellQuest software.

To measure RSV-specific CD8$^+$ T cells in PBMC of adult volunteers, CFSE (Sigma-Aldrich)-labeled PBMC were cultured with synthetic peptide at 1 μM for 6 days in the presence of 20 U/ml of recombinant human IL-2. CFSE labeling of PBMC was performed during 5 min at room temperature in 2.5 mM CFSE in serum-free culture medium. Cells were washed three times in culture medium with 10% FCS before culture with peptide. At day 6, RSV-specific CD8$^+$ T cells were visualized by staining with HLA tetrameric complexes, in a gate for live cells (based on forward/side scatter) that had divided (based on dilution of CFSE). Percentages of tetramer-positive cells as a fraction of total CD8$^+$ cells are depicted in the figures. All PBMC samples of an individual were tested in one experiment.

Statistics

Comparison of differences between patient groups (i.e., infected with RSV or rhinovirus) was made using the Mann-Whitney *U* test. A *p*-value of <0.05 was considered significant. Statistical analysis of the data in Fig. 1 was performed by using two-tailed Student's *t* test (GraphPad Prism). Values are expressed as the means ± SEM.

Results

During respiratory viral infections, bystander CD8$^+$ T cells specific for different respiratory viruses disappear from blood

Upon primary infection with RSV, both an Ab response and CD8$^+$ T cell immunity against well-conserved epitopes develop. However, despite the memory B and T cell responses, reinfections in healthy adults occur regularly (1). To evaluate the dynamics of RSV-specific T cell memory during common respiratory infections, we followed 10 healthy volunteers during the winter season. Each week blood was drawn and nose/throat swabs were taken to check for the presence of viruses. Eight of 10 individuals experienced at least one episode of common cold. In five individuals the virus was identified. Unfortunately, we did not find RSV. However, as sampling was performed only once a week, viral detection was not optimal.

After collection of all the blood samples, the RSV-specific memory CD8$^+$ T cell response was investigated. Because we had previously found that RSV-specific CD8$^+$ T cells specific for single RSV epitopes were present at low frequencies (19), CFSE-labeled PBMC were cultured with synthetic peptides for 6 days. On day 6 the presence of RSV-specific CD8$^+$ T cells was determined by tetramer staining in the cell population with low CFSE, that is, the cells that had divided in the cultures. In all patients with either clinical symptoms or asymptomatic infection we observed a reduction of RSV-specific cells during respiratory infection (representative examples shown in Fig. 1*A–D*).

Determination of exact frequencies of RSV-specific memory CD8$^+$ T cells was impossible because of the in vitro expansion that was necessary to visualize RSV-specific T cells. To investigate the disappearance of virus-specific CD8$^+$ T cells during infections with heterologous viruses without the need of in vitro expansion, we also determined the influenza virus-specific T cell numbers that are present in higher frequencies in peripheral blood (5). In these experiments we performed direct staining in four HLA-A2-positive donors with HLA-A2 tetrameric complexes containing peptide $M1_{58-66}$ derived from the influenza matrix protein. At several time points before, during, and after the onset of clinical symptoms of respiratory infection, blood samples of HLA-A2-positive donors were collected. We found a reduction but not complete disappearance of $M1_{58-66}$-specific CD8$^+$ T cells in peripheral blood during clinical symptoms caused by unrelated respiratory viruses (Fig. 1, *E* and *F*). The percentage of influenza virus-specific cells in peripheral blood was restored between day 4 and 7 after the onset of symptoms during heterologous infections. In the experiments described so far we have used tetramer staining to positively identify CD8$^+$ T cells specific for virus-derived epitopes. However, the frequency of CD8$^+$ T cells specific for single viral epitopes is low in peripheral blood. Therefore, we performed additional experiments using the ELISPOT assay for IFN-γ. PBMC were stimulated with live virus to display the peptide repertoire representing the entire proteome of the virus. Fig. 1, *G* and *H*, shows the diminished RSV-specific T cell response during upper respiratory tract infection. Using a mixture of HLA-DR-, HLA-DQ-, and HLA-DP-blocking Abs in this assay allowed us to evaluate the effect on CD8$^+$ T cells only. CD8$^+$ T cell numbers specific for RSV were detected in lower numbers in peripheral

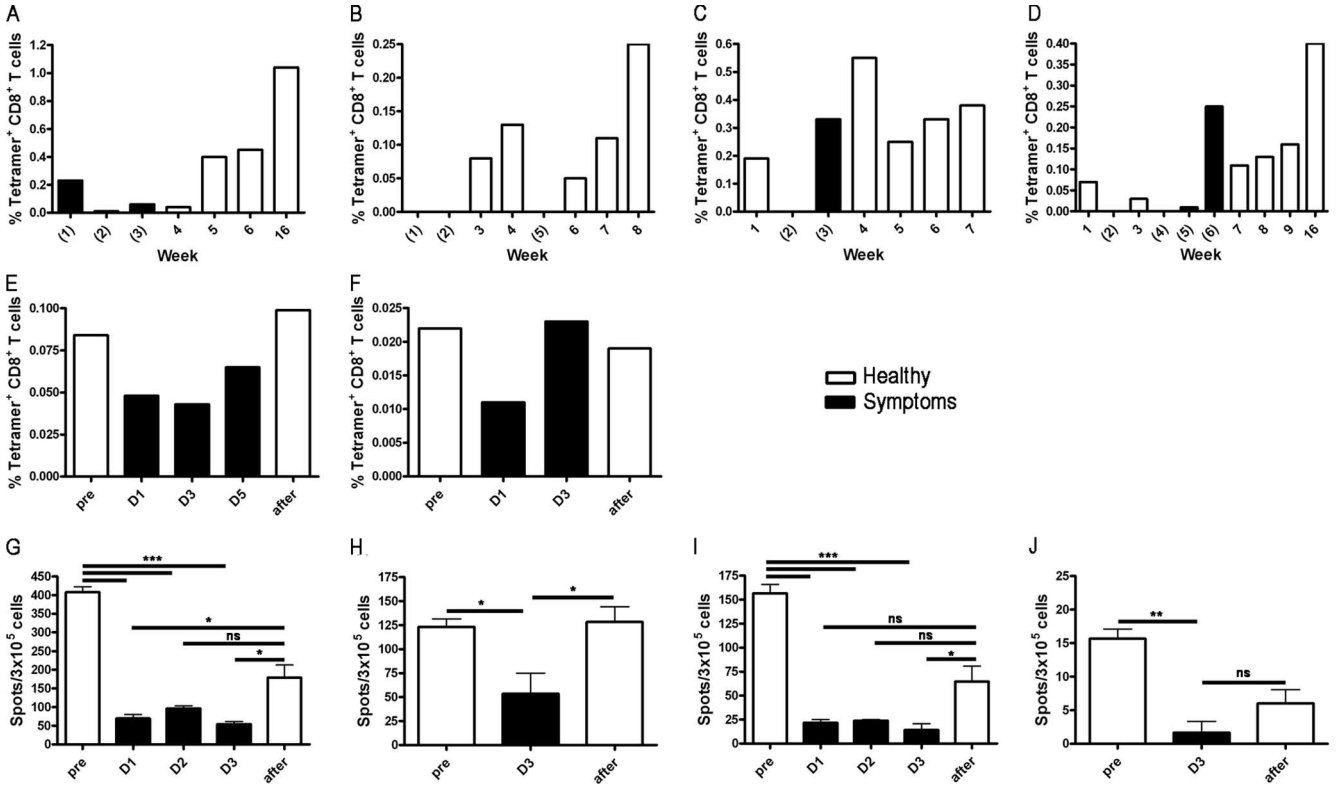

FIGURE 1. Dynamics of virus-specific CD8$^+$ T cell numbers in peripheral blood during episodes of respiratory infections in adults. *A–D*, RSV-specific CD8$^+$ T cells. CFSE-labeled PBMC of healthy blood donors were stimulated for 6 days with peptide in the presence of IL-2. On day 6 cells were stained with the appropriate HLA tetramer. Cells were gated based on negative 7-aminoactinomycin D staining and positive CD8 staining. The percentage of tetramer-positive CFSE-negative cells of total CD8$^+$ T cells is given for each time point. *A*, PBMC of an HLA-A1-positive individual stimulated with the peptide YLEKESIYY (RSV-$M_{229-237}$). PCR in nose/throat swab samples showed a coronavirus infection in week 1 and an influenza virus infection in week 2. *B*, PBMC of an HLA-A3-positive individual stimulated with the peptide RLPADVLKK (RSV-$M2_{151-159}$). This donor experienced symptoms of a respiratory infection in weeks 1, 2, and 5. No virus was identified in nose/throat swabs at all time points. *C* and *D*, Two HLA-A1-positive donors were stimulated with YLEKESIYY (RSV-$M_{229-237}$). For the donor represented in *C*, influenza virus was detected in week 2. The donor represented in *D* experienced symptoms of a respiratory infection in weeks 2 and 4–6. PCR of the nose/throat swab sample was negative in week 2, and rhinovirus was detected in week 4. Filled bars and parentheses around week numbers indicate that the individual had symptoms of a respiratory infection on the day of specimen collection. The four donors are representative of 8 of 10 individuals who experienced symptoms during the study period. *E* and *F*, Influenza-specific CD8$^+$ T cells in PBMC during respiratory virus infections. PBMCs of two HLA-A2-positive donors were stained with a HLA-A2 tetramer loaded with the influenza virus peptide $M1_{58-66}$ (GILGFVFTL). Samples were taken 2 wk before, and on several time points after, onset of clinical symptoms and after resolution of the infection. The donor represented in *E* had a rhinovirus infection. The second donor, shown in *F*, had cold symptoms but no virus was identified. *G–J*, IFN-γ ELISPOT assay performed with PBMC of two donors with upper respiratory tract infections. The infecting virus was not identified in these subjects. PBMC were stimulated with RSV strain A2 at a moi of 5. *G* and *H* represent the number of spots per 3×10^5 PBMC of two different donors. *I* and *J* are the T cell responses of the same donors when the experiment was performed in the presence of HLA-DR/DQ/DP-blocking Abs and therefore show the response of CD8$^+$ T cells only. D1, D2, D3, and D5 depict the day after the first symptoms, before and after samples were taken 6 wk before the onset of first symptoms and 6 wk after. ns, not significant; *, $p < 0.05$; **, $p < 0.01$; ***, $p < 0.001$.

blood during upper respiratory infections similar to the diminished number of CD8$^+$ T cells using tetramer staining (Fig. 1, *I* and *J*.). Using the ELISPOT assay, similar results were found in two donors for T cell responses against influenza virus (data not shown).

In most donors the number of PBMC recovered was lower during infection, and the percentage of CD8$^+$ T cells within the CD3$^+$ cell population decreased. Therefore, it appeared that the absolute number of RSV and influenza virus-specific cells also decreased. These results suggested the efflux from the blood of CD8$^+$ T cells directed against respiratory viruses during episodes of upper respiratory tract infection.

A significant increase in CD8$^+$ T cells with an effector (CD127$^-$) phenotype is found in PBMC of adults with common colds

CD8$^+$ T cells directed against a single epitope of influenza virus obviously represent only a minor part of the memory pool of T cells directed against respiratory viruses. Therefore, we next analyzed the dynamics of the entire CD8$^+$ T cell population in blood. During upper respiratory tract infection the percentage of activated effector cells, CD45RO$^+$, CCR7$^-$ CD127$^-$, and HLA-DR$^+$ cells increased (Fig. 2). The peak of the response was found on days 3–7 after the onset of symptoms. The expression of chemokine receptor CCR5 on these cells indicated their capacity to migrate into the inflamed lung.

During respiratory infections there is an influx of proliferating highly activated CD8$^+$ T cells into the airways

During infection with a respiratory virus the airway epithelium is the tissue where viral Ags are expressed and innate immune responses create an inflammatory environment attracting effector T cells. To study whether the activated effector cells migrated from blood to the airways, we followed CD8$^+$ T cell responses in the large airways during respiratory infection.

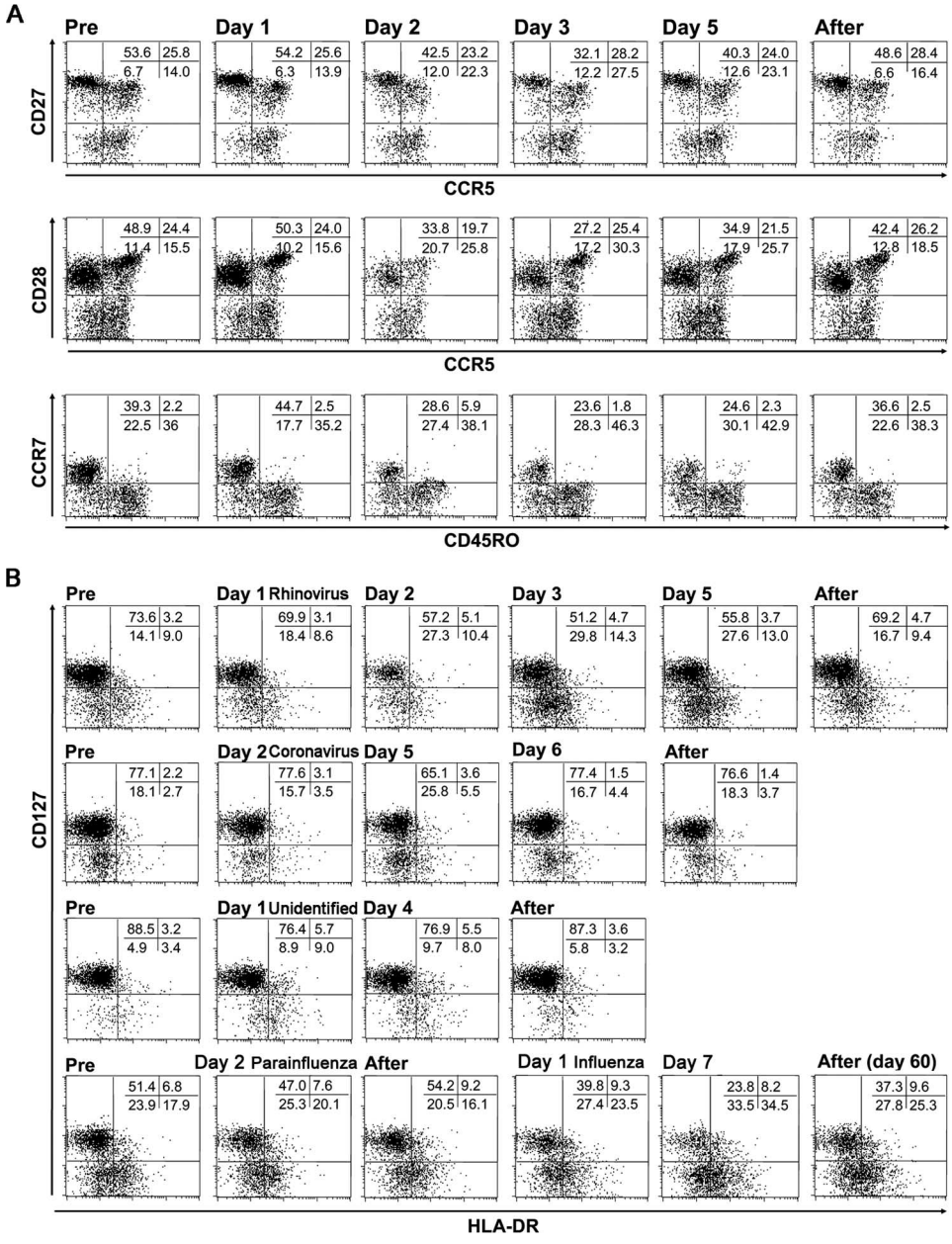

FIGURE 2. *A*, Dynamics of the $CD8^+$ T cell population in blood during rhinovirus infection. PBMC of an adult donor were collected 2 wk before, on several days after onset of symptoms, and 2 mo after resolution of the infection and stained for differentiation and activation markers. Similar results were obtained in three additional donors. *B*, Decrease in naive/memory $CD8^+$ T cell populations ($CD127^+$) and increase in effector population ($CD127^-$) shown in four donors with respiratory infections. Day 1 is the first day of cold symptoms. Cells were gated for live $CD8^+$ T cells based on forward/side light scatter.

Fifteen children between 6 mo and 18 years of age with a tracheostoma were followed during one winter season. On days 2, 5, 8, 15, 28, and 56 after the onset of symptoms of a respiratory infection, the $CD8^+$ T cell number and phenotype were measured in tracheal aspirate. In these children, 21 episodes of upper respiratory tract infection were studied (Table I). In the first 3–5 days after the onset of respiratory symptoms we found a higher ratio of $CD8^+$ vs $CD4^+$ T cells than later in the response when symptoms diminished and eventually disappeared (Fig. 3*A*). Moreover, early after the onset of symptoms a higher proportion of $CD8^+$ T cells expressed the activation marker HLA-DR than later in the response (Fig. 3*B*). While in almost all patients >70% of $CD8^+$ T cells expressed the cytotoxicity marker GzmB during infection, the basic level of GzmB expression after 28 days varied tremendously among patients (between 10% and 70%; data not shown). The number of T cells expressing perforin, another component of cytotoxic granules, declined much faster and <10% of $CD8^+$ T cells was found positive on day 30 (Fig. 3*C*). Proliferating $CD8^+$ T cell numbers visualized by Ki-67 staining peaked between day 2 and 5, with up to 30% proliferating $CD8^+$ T cells (Fig. 3*D*). In all patients, CCR5, CD45RO, and CD27 were expressed in >75% of $CD8^+$ T cells at all time points. Twenty-five to 50% of $CD8^+$ T cells expressed CD28. CD25 and CCR7 were expressed by <5% of $CD8^+$ T cells. No variation in these values was found at the different time points of sampling (data not shown).

$CD8^+$ T cells show higher rates of proliferation and activation during infections with RSV than during rhinovirus infection

To study the role of $CD8^+$ T cells during infections with different viruses, we compared T cell responses in children infected with RSV (three children, mean age 4.2 years) and rhinovirus infections (seven children, mean age 6.8 years). At the peak of the response, RSV-infected children had a higher influx of $CD8^+$ T cells into the airways and significantly lower percentages of $CD4^+$ T cells, resulting in lower CD4/CD8 ratios (Fig. 4, *A* and *B*). The number of proliferating (Ki-67^+) $CD8^+$ T cells and the number of cells expressing GzmB or CD38 were

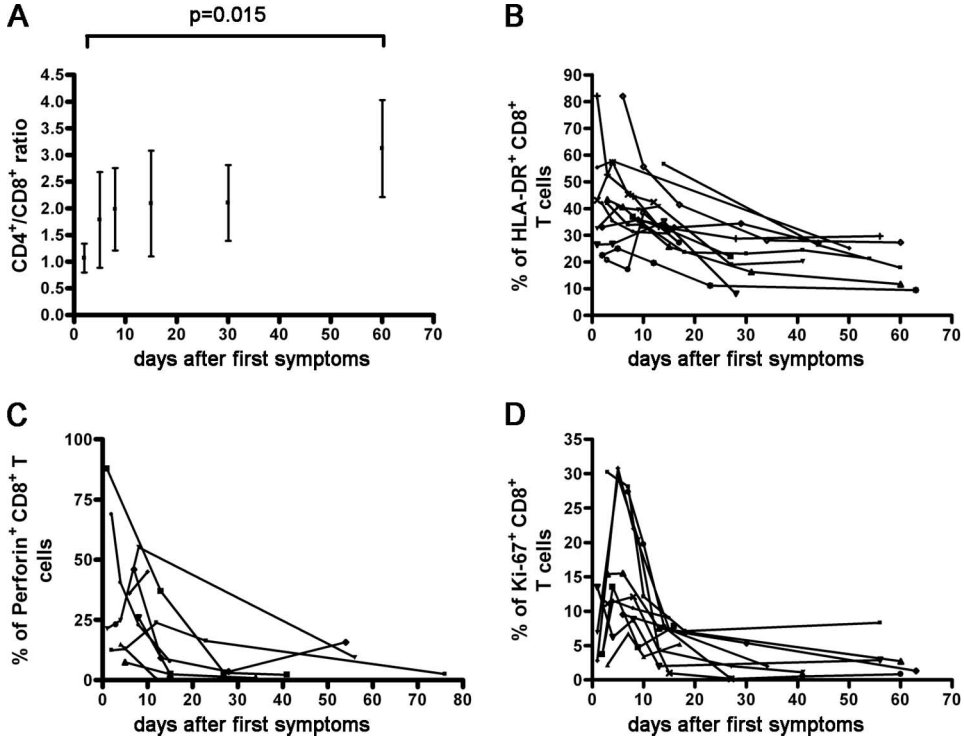

FIGURE 3. Activation status of CD8$^+$ T cells in tracheal aspirates of children with symptoms of respiratory infections. In 15 children (Table I) tracheal aspirate was collected at six time points after onset of symptoms. Cells of tracheal aspirate were stained for several activation markers. Missing values are either due to interfering new infections or limited numbers of cells in the aspirate.

significantly higher during RSV infection (Fig. 4*C*). In one child with four consecutive infections (rhinovirus, RSV, coronavirus, and rhinovirus), we observed more proliferating CD8$^+$ T cells during RSV and coronavirus infection than during two rhinovirus infections, while the response was comparable between the two rhinovirus infections (Fig. 4*D–F*).

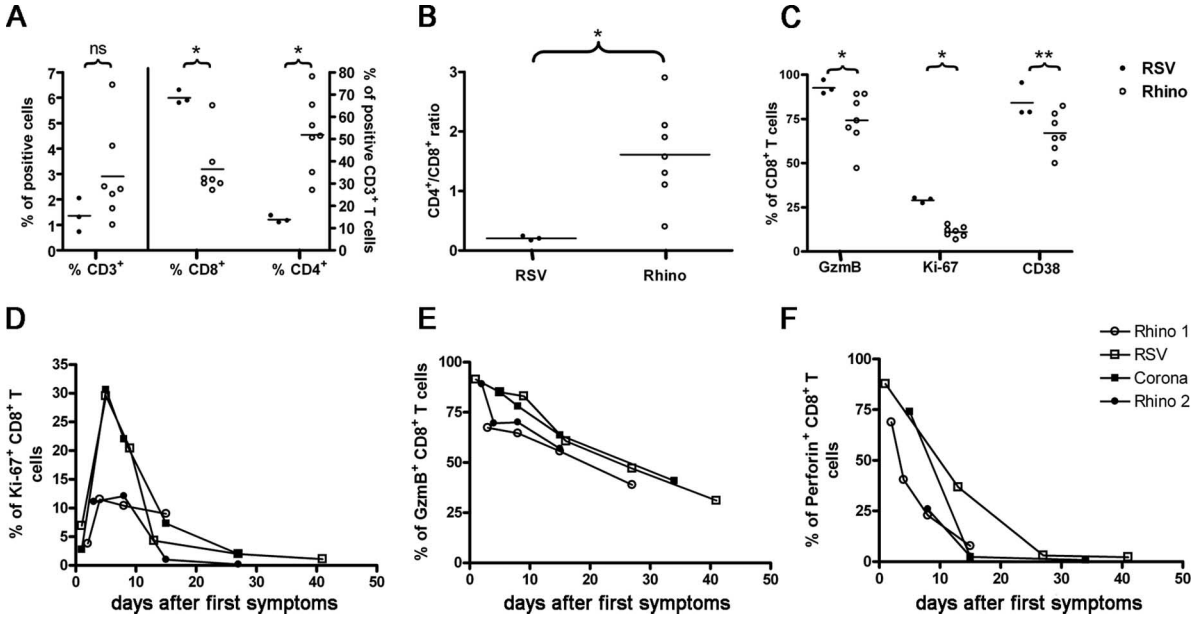

FIGURE 4. Comparison of T lymphocyte populations in tracheal aspirate samples during RSV (patients 5, 9, and15) and rhinovirus (patients 2, 8, 9-2x), 11, 12, and 13) infections. *A*, Percentage of CD3$^+$ lymphocytes of total cells in tracheal aspirate of patients infected with RSV (●) and rhinovirus (○). CD4$^+$ and CD8$^+$ T cells are depicted as the percentage of total live CD3$^+$ cells in tracheal aspirates. *B*, Comparison of CD4/CD8 ratio in these patients. *C*, Activation markers on CD8$^+$ T cells present in tracheal aspirate samples of RSV- and rhinovirus-infected patients. The values depicted are from the samples taken at the peak of the response usually day 2 or 5 after the onset of symptoms. Percentages of marker-positive live CD8$^+$ T cells are shown, based on negative 7-aminoactinomycin D staining and positive CD8$^+$ staining. *, $p < 0.02$; **, $p < 0.05$; ns, not significant. *D–F*, Activation markers on CD8$^+$ T cells in tracheal aspirate of a 5-year-old patient (no. 9, Table I) who suffered from four consecutive respiratory infections, respectively: rhinovirus (○), RSV (□), coronavirus (■), and rhinovirus (●). Cells were gated on a CD8$^+$ and live lymphocyte gate based on the forward/side light scatter.

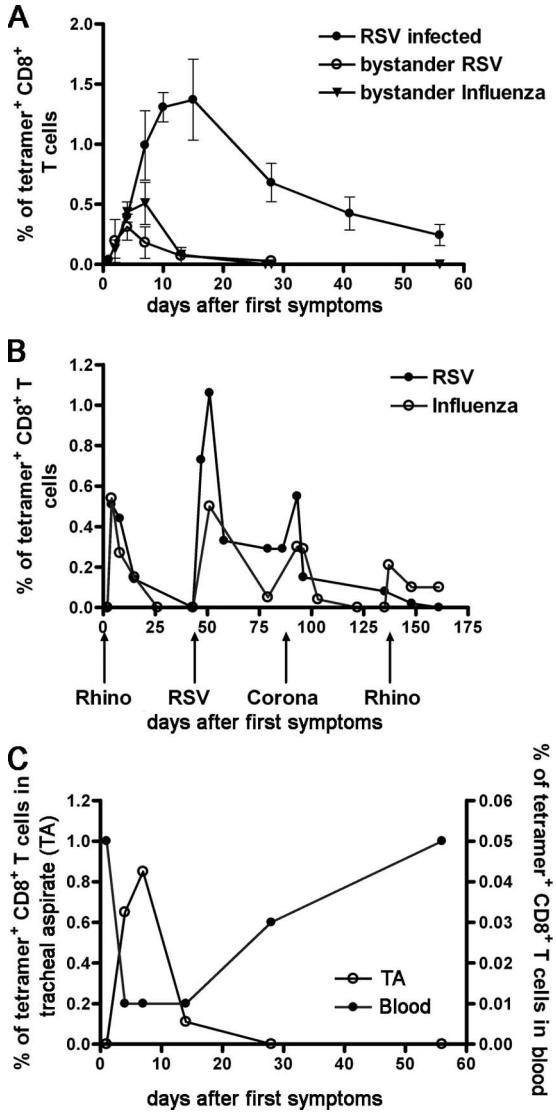

FIGURE 5. Migration of virus-specific and bystander T cells to the airways. *A*, Percentages of RSV-specific HLA tetramer-positive (HLA-A1/$M_{229-237}$, HLA-A3/$M2_{151-159}$, and HLA-B7/$NP_{306-314}$) $CD8^+$ T cells in tracheal aspirates of five patients (Table I: patient 1, HLA-A1; patient 3, HLA-A3; patient 5, HLA-A3; patient 9, HLA-B7; and patient 15, HLA-A1) with RSV infections (●), four patients with different infections, three with rhinovirus infection (patient 2, HLA-A1; patient 9, HLA-B7; and patient 13, HLA-A1) and one with coronavirus infection (patient 9, HLA-B7) (○), and influenza-specific HLA-A2/$M1_{58-66}$ or HLA-A1/Np_{44-52} tetramer-positive $CD8^+$ T cells during six episodes of viral infection, four with rhinovirus (patient 9-2x), HLA-A2; patient 13, HLA-A1; and patient 12, HLA-A2), one coronavirus (patient 9, HLA-A2), and one RSV infection (patient 9, HLA-A2) (▼). The percentage of tetramer-positive cells of total live $CD8^+$ T cells is shown. *B*, In one patient (Table I, patient 9) with four consecutive infections, RSV- and influenza virus-specific $CD8^+$ T cells were identified in tracheal aspirate by tetramer staining (HLA-A2/influenza-$M1_{58-66}$ and HLA-B7/RSV-$NP_{306-314}$). *C*, Influenza virus-specific cells appear in tracheal aspirate at the same time they disappear from blood. At six time points after onset of symptoms due to rhinovirus infection, PBMC and tracheal aspirate of an HLA-A2-positive patient (no. 9, Table I) were stained with HLA-A2/influenza-$M1_{58-66}$ tetrameric complexes. In all figures the percentages of tetramer-positive cells of total live $CD8^+$ T cells are shown.

Bystander $CD8^+$ T cells are recruited to the airways during viral respiratory infections

We next tested the specificity of $CD8^+$ T cells attracted to the airways using HLA tetrameric complexes. HLA tetramers containing antigenic peptides derived from RSV and influenza virus proteins were applied in HLA-A1-, HLA-A2-, HLA-A3-, or HLA-B7-positive donors. Patients were followed during several episodes of respiratory infections. RSV-specific $CD8^+$ T cell responses were studied during three infections with rhinovirus, one infection with coronavirus, and three infections with RSV. The influenza-specific $CD8^+$ T cell response was studied during four episodes of rhinovirus, one coronavirus, and one RSV infection. During each episode, influenza virus and/or RSV-specific $CD8^+$ T cells appeared in tracheal aspirate. T cell numbers peaked before day 10 after the onset of symptoms and disappeared soon thereafter (Fig. 5*A*). In one child with four episodes of common cold, virus-specific T cells appeared with every episode and T cell numbers declined in symptom-free periods (Fig. 5*B*). Peak responses against single epitopes, measured by tetramer staining, varied between 0.1 and 0.83 of $CD8^+$ T cells. In one child with a rhinovirus infection we were able to compare the level of influenza tetramer-positive cells simultaneously in tracheal aspirate and blood. Although the percentage of influenza virus-specific $CD8^+$ T cells was much lower in blood than in the airways, we found that similar to observations described in Fig. 1, influenza virus-specific cells disappeared from blood. When the cells disappeared from the peripheral blood they appeared in tracheal aspirate (Fig. 5*C*). Thus, $CD8^+$ T cells specific for respiratory viruses appear to be attracted to the airways during unrelated respiratory infections, which results in a temporary decline in peripheral blood. During infection with RSV the number of RSV-specific $CD8^+$ T cells in tracheal aspirate exceeded levels during infection with other viruses. When RSV-specific $CD8^+$ T cell responses were compared between children with RSV infection and other viral infections, the magnitude was higher and elevated virus-specific cell numbers were present for a longer period in RSV-infected individuals (Fig. 5*A*). Similar observations were made for influenza virus-specific responses (data not shown). Thus, secondary antiviral $CD8^+$ T cell responses are of higher magnitude and of longer duration than are bystander responses during unrelated infections.

Discussion

The observations made in the present study in human patients showed that in the circulation significant shifts in $CD8^+$ T cell populations occur during mild upper respiratory infections. All three phases of the T cell responses observed during murine respiratory infections, reflecting three waves of different populations of memory cells contributing to the response in the airways, could be recognized in our experiments (20, 21). The first phase is represented by effector/memory $CD8^+$ T cells that are already present in the lungs. Indeed, long after clearance of a respiratory infection, cells present in tracheal aspirate are of the effector/memory type. These cells reflect the effector/memory cells already present before the next exposure to a respiratory pathogen. The second phase of memory cells that are attracted to the inflammatory site in our experiments are identified as influenza virus-specific cells and RSV-specific cells recruited during heterologous respiratory infections (Fig. 5, Refs. 9, 22, 23). Indeed, as it was described in the murine model, this non-specific response, composed of effector/memory cells that originated from T cell pools present in the circulation, waned faster than did the virus-specific response during homologous infections (9, 13). While during heterologous infection RSV-specific cells disappeared from the airways within 2 wk, during secondary RSV infection RSV-specific $CD8^+$ T cell responses peaked later and the virus-specific cells remained detectable at higher

than initial levels up to 58 days (Fig. 5*A*). The sustained response of virus-specific CD8$^+$ T cells during homologous infections is caused by the contribution of memory cells that encounter APCs in the lymph nodes draining the infection site (20). This induces T cell proliferation and effector function and the ability to migrate to the inflammatory site. These cells of the third wave are more apoptosis resistant than are nonspecific bystanders due to exposure to cognate Ag (21). Furthermore, a prolonged presence of APCs that display viral Ags in the draining lymph nodes has been documented to be involved in a sustained specific antiviral response (15). However, this prolonged Ag presentation might be less pronounced during secondary infections when infectious material is rapidly cleared and lower viral loads are reached. The observation that the influx of dividing (i.e., Ki-67$^+$) cells decreased in the airways before day 10 (Fig. 3*D*) while peak RSV-specific CD8$^+$ T cell numbers did not decline until day 15 (Fig. 5*A*) may indicate that prolonged survival times determined longer persistence of specific T cells during homologous infections.

It has been suggested that bystander recruitment early during respiratory viral infection is the result of the proinflammatory milieu at the site of infection created by the secretion of several cytokines and chemokines (9). The rapid recruitment of all T cells to the site of inflammation provides a fast defense to previously experienced infections and enables crossreactive CD8$^+$ T cells to contribute in heterologous infections. After recruitment to the airways, these bystander cells are presumably lost by apoptosis or phagocytosis, as in the mouse it has been shown that lung airway memory T cells are unable to migrate from the airways back into the circulation in contrast to T cells present in the lung interstitium (9, 4, 13, 24). In our study we showed that virus-specific memory T cells reappear in blood after disappearance from the airways. At present, we do not know whether in humans these CD8$^+$ T cells migrated back from the airways, were redistributed from other sites, or were replenished by proliferation.

Compared with children with rhinovirus infections, we found higher fractions of CD8$^+$ T cells in the airways expressing GzmB, Ki-67, and CD38 in children infected with RSV. This might be due to the fact that all children with RSV infection were more severely ill than were children with rhinovirus infection.

The possibility to obtain tracheal aspirate at different time points after infection provided a unique opportunity to study developing secondary immune responses at the local infection site. Using HLA tetrameric complexes we were able to study the dynamics of CD8$^+$ T cells with particular specificities. However, due to the fact that the single epitopes used in the HLA tetrameric complexes only represent a small fraction of virus-specific cells and the number of cells recovered from tracheostomal aspirates was low, it was impossible to obtain a full phenotypic characterization of the virus-specific T cells that migrated to the lungs. Moreover, studies in patients will always have the disadvantage that the experimental setup cannot be controlled. Therefore, the exact time of virus inoculation was unknown, as was the viral load at the time of infection. Furthermore, the patient group was heterogeneous with respect to age and underlying disease condition and the history of unknown previous respiratory infections. We excluded children with immune disorders and children using immune suppressive medication to avoid immunological aspects of underlying diseases as much as possible. Due to the fact that the tracheostoma is an open connection between the outside environment and the trachea, the lower respiratory tract of tracheostoma patients is continuously exposed to bacterial infections. About 95% of tracheostoma openings in adults contain bacterial colonization, while in 30–46% of deeper brush cultures bacterial growth was found (25, 26). It has previously been shown that this results in a persistent baseline inflammation. Compared with healthy controls there is a larger influx of neutrophils in tracheostoma patients. Nevertheless, the tracheostoma patients provided us with unique material that is impossible to obtain from healthy individuals, and the observations made provided valuable information on the dynamics of secondary T cell responses at the local infection site during the course of a respiratory infection. In summary, these studies provide insight in human T cell dynamics upon viral infections. Studying human T cell responses in both peripheral and central sites will contribute to a broader understanding of the complex human T cell immunology necessary for future development of vaccines.

Acknowledgments

The authors thank all patients, parents, and blood donors for their cooperation. We also thank Dr. Anne Schilder, Dr. Mike J. Kampelmacher, Dr. Rob G. van Kesteren, and Prof. Adrianus J. van Vught for their help with the inclusion of patients. Mariska E. A. van Dijk and Laura van Drie are thanked for technical assistance, and Prof. Frank Miedema and Dr. Beate Kampmann for reading the manuscript.

Disclosures

The authors have no financial conflicts of interest.

References

1. Hall, C. B., C. E. Long, and K. C. Schnabel. 2001. Respiratory syncytial virus infections in previously healthy working adults. *Clin. Infect. Dis.* 33: 792–796.
2. Hashem, M., and C. B. Hall. 2003. Respiratory syncytial virus in healthy adults: the cost of a cold. *J. Clin. Virol.* 27: 14–21.
3. Liang, S., K. Mozdzanowska, G. Palladino, and W. Gerhard. 1994. Heterosubtypic immunity to influenza type A virus in mice: effector mechanisms and their longevity. *J. Immunol.* 152: 1653–1661.
4. Galkina, E., J. Thatte, V. Dabak, M. B. Williams, K. Ley, and T. J. Braciale. 2005. Preferential migration of effector CD8$^+$ T cells into the interstitium of the normal lung. *J. Clin. Invest.* 115: 3473–3483.
5. de Bree, G. J., J. Heidema, E. M. van Leeuwen, G. M. van Bleek, R. E. Jonkers, H. M. Jansen, R. A. van Lier, and T. A. Out. 2005. Respiratory syncytial virus-specific CD8$^+$ memory T cell responses in elderly persons. *J. Infect. Dis.* 191: 1710–1718.
6. Ostler, T., T. Hussell, C. D. Surh, P. Openshaw, and S. Ehl. 2001. Long-term persistence and reactivation of T cell memory in the lung of mice infected with respiratory syncytial virus. *Eur. J. Immunol.* 31: 2574–2582.
7. Powell, T. J., D. M. Brown, J. A. Hollenbaugh, T. Charbonneau, R. A. Kemp, S. L. Swain, and R. W. Dutton. 2004. CD8$^+$ T cells responding to influenza infection reach and persist at higher numbers than CD4$^+$ T cells independently of precursor frequency. *Clin. Immunol.* 113: 89–100.
8. Lawrence, C. W., R. M. Ream, and T. J. Braciale. 2005. Frequency, specificity, and sites of expansion of CD8$^+$ T cells during primary pulmonary influenza virus infection. *J. Immunol.* 174: 5332–5340.
9. Ely, K. H., L. S. Cauley, A. D. Roberts, J. W. Brennan, T. Cookenham, and D. L. Woodland. 2003. Nonspecific recruitment of memory CD8$^+$ T cells to the lung airways during respiratory virus infections. *J. Immunol.* 170: 1423–1429.
10. Selin, L. K., S. M. Varga, I. C. Wong, and R. M. Welsh. 1998. Protective heterologous antiviral immunity and enhanced immunopathogenesis mediated by memory T cell populations. *J. Exp. Med.* 188: 1705–1715.
11. Chen, H. D., A. E. Fraire, I. Joris, M. A. Brehm, R. M. Welsh, and L. K. Selin. 2001. Memory CD8$^+$ T cells in heterologous antiviral immunity and immunopathology in the lung. *Nat. Immunol.* 2: 1067–1076.
12. de Bree, G. J., E. M. van Leeuwen, T. A. Out, H. M. Jansen, R. E. Jonkers, and R. A. van Lier. 2005. Selective accumulation of differentiated CD8$^+$ T cells specific for respiratory viruses in the human lung. *J. Exp. Med.* 202: 1433–1442.
13. Hogan, R. J., E. J. Usherwood, W. Zhong, A. A. Roberts, R. W. Dutton, A. G. Harmsen, and D. L. Woodland. 2001. Activated antigen-specific CD8$^+$ T cells persist in the lungs following recovery from respiratory virus infections. *J. Immunol.* 166: 1813–1822.
14. Schluns, K. S., W. C. Kieper, S. C. Jameson, and L. Lefrançois. 2000. Interleukin-7 mediates the homeostasis of naive and memory CD8 T cells in vivo. *Nat. Immunol.* 1: 426–432.
15. Zammit, D. J., D. L. Turner, K. D. Klonowski, L. Lefrançois, and L. S. Cauley. 2006. Residual antigen presentation after influenza virus infection affects CD8 T cell activation and migration. *Immunity* 24: 439–449.
16. Doerschuk, C. M. 2000. Leukocyte trafficking in alveoli and airway passages. *Respir. Res.* 1: 136–140.
17. van de Pol, A. C., A. M. van Loon, T. F. Wolfs, N. J. Jansen, M. Nijhuis, E. K. Breteler, R. Schuurman, and J. W. Rossen. 2007. Increased detection of

respiratory syncytial virus, influenza virus, parainfluenza viruses and adenoviruses with real-time PCR in samples from patients with respiratory symptoms. *J. Clin. Microbiol.* 45: 2260–2262.
18. van Doornum, G. J., J. Guldemeester, A. D. Osterhaus, and H. G. Niesters. 2003. Diagnosing herpesvirus infections by real-time amplification and rapid culture. *J. Clin. Microbiol.* 41: 576–580.
19. Heidema, J., G. J. de Bree, P. M. de Graaff, W. W. C. van Maren, P. Hoogerhout, T. A. Out, J. L. Kimpen, and G. M. van Bleek. 2004. Human $CD8^+$ T cell responses against five newly identified respiratory syncytial virus-derived epitopes. *J. Gen. Virol.* 85: 2365–2374.
20. Hikono, H., J. E. Kohlmeier, K. H. Ely, I. Scott, A. D. Roberts, M. A. Blackman, and D. L. Woodland. 2006. T-cell memory and recall responses to respiratory virus infections. *Immunol. Rev.* 211: 119–132.
21. Woodland, D. L., and I. Scott. 2005. T cell memory in the lung airways. *Proc. Am. Thorac. Soc.* 2: 126–131.
22. Masopust, D., V. Vezys, E. J. Usherwood, L. S. Cauley, S. Olson, A. L. Marzo, R. L. Ward, D. L. Woodland, and L. Lefrançois. 2004. Activated primary and memory CD8 T cells migrate to nonlymphoid tissues regardless of site of activation or tissue of origin. *J. Immunol.* 172: 4875–4882.
23. Topham, D. J., M. R. Castrucci, F. S. Wingo, G. T. Belz, and P. C. Doherty. 2001. The role of antigen in the localization of naive, acutely activated, and memory $CD8^+$ T cells to the lung during influenza pneumonia. *J. Immunol.* 167: 6983–6990.
24. Harris, N. L., V. Watt, F. Ronchese, and G. G. Le. 2002. Differential T cell function and fate in lymph node and nonlymphoid tissues. *J. Exp. Med.* 195: 317–326.
25. Harlid, R., G. Andersson, C. G. Frostell, H. J. Jorbeck, and A. B. Ortqvist. 1996. Respiratory tract colonization and infection in patients with chronic tracheostomy: a one-year study in patients living at home. *Am. J. Respir. Crit. Care Med.* 154: 124–129.
26. Cabello, H., A. Torres, R. Celis, M. El Ebiary, D. L. B. Puig, A. Xaubet, J. Gonzalez, C. Agusti, and N. Soler. 1997. Bacterial colonization of distal airways in healthy subjects and chronic lung disease: a bronchoscopic study. *Eur. Respir. J.* 10: 1137–1144.